

Filtering methods to extract the tide height from Global Navigation Satellite Systems (GNSS) signals for Hydrographic applications

Faisal ALSAAQ, Michael KUHN, Ahmed EL-MOWAFY & Paul KENNEDY

Key words: Hydrography, GNSS, tidal harmonic constituents, spectral analysis, Bathymetry

ABSTRACT

Hydrographic surveys have traditionally relied on the availability of tide information for the reduction of sounding observations to a common (chart) datum usually related to a specific tide level. In most cases, tide information is obtained from tide gauge observations and/or tide predictions using local, regional or global tide models. An emerging method that is increasingly being used is based on Global Navigation Satellite System (GNSS) positioning of the sea surface. This study assesses the suitability of two types of filtering methods to extract the tide signal from GNSS height observations of the water level. The Savitzky-Golay and Gaussian low-pass filters were implemented to eliminate high-frequency components due to waves, dynamic draft and measurement uncertainties. Over a 30-day period, GNSS heights were estimated from GPS and GLONASS carrier phase data collected by a Fugro Starpack GNSS receiver installed on a floating pontoon at Hillarys Boat Harbor, located in Western Australia. Sea level heights recorded by a traditional tide gauge at Hillarys were used as a reference to evaluate the effectiveness of using GNSS water level heights in extracting the tide signal. To assess the filters performance for a range of window lengths, amplitudes and phases of the four major tidal harmonic constituents (M₂, S₂, K₁, and O₁) were determined and compared for the unfiltered and filtered water level signals. The study found a high degree of agreement between the unfiltered tide information obtained by GNSS and the tide gauge documented by almost identical amplitudes of the tidal harmonic constituents. There was a correlation coefficient of up to 0.98 and an RMS value of 0.0325 m for the differences satisfying specifications of the International Hydrographic Organization (IHO) for Special Order hydrographic surveys. As a main finding regarding the filter performance, this study shows that the Savitzky-Golay filter suffers considerably less from signal loss (damping of the tidal harmonic constituents) when compared to the Gaussian filter.

1. INTRODUCTION

In hydrographic surveying, the reduction of tide variations from acoustic depth observations is an important aspect as it is used to reduce the water depth observations to a common datum (e.g. chart datum). In the past, tide reductions were typically derived from data recorded by tide gauges located close to the survey area. Recent advances in satellite positioning have seen an increased use of GNSS in oceanographic applications such as the derivation of tide information (Tay, Coatanhay, Maussang, & Garello, 2010). Today, GNSS positioning is often used in hydrographic surveys due to the ability to estimate three-dimensional positions (e.g. horizontal

Page | 1

Faisal ALSAAQ, Michael KUHN, Ahmed EL-MOWAFY & Paul KENNEDY

Filtering methods to extract the tide height from Global Navigation Satellite Systems (GNSS) signals for Hydrographic applications

HYDRO 2016

Rostock-Warnemünde, Germany, 08 – 10 November 2016

position and height). While the horizontal positions from GNSS are commonly used today, a particular focus of hydrographers is on the vertical component providing information on water level changes. In addition, a benefit of GNSS vertical positioning is that the objects in question (e.g. sea surface, water column, sea floor, etc.) are referenced directly (both horizontally and vertically) to a geometrically defined reference ellipsoid without the need for further external information (Mills & Dodd, 2014).

Many studies have analysed different methods to extract tidal frequencies from tide height records predominantly based on Fourier and wavelet analyses. For example, Flinchem and Jay (2000) and Jay and Kukulka (2003) considered tide time series to be non-stationary and introduced the continuous wavelet transform (CWT) method, a complementary technique to harmonic analysis and Fourier methods, to extract tidal information. Ducarme, Venedikov, Arnoso, & Vieira, (2006) used a method based on maximum likelihood estimates known as the Akaike Information Criterion (AIC) method (Sakamoto, Ishiguro, & Kitagawa, 1986) to find non-tidal components in tidal residuals obtained after reduction of tidal harmonic constituents through a computer program, known as VAV (Venedikov, Arnoso, & Vieira, 2005). Pytharouli and Stiros (2012) applied spectral analysis to the time series of the astronomical tide (smoothed tide time series) based on the NormPeriod code. Filtering methods have been used to smooth tidal data, where filters suppress high-frequency variations in the observation data and disclose lower-frequency (longer-period) tidal signals. Nevertheless, application of filters to tidal variations is rather limited (e.g., Lam, 1974; Wert, Dare, & Clarke, 2004).

In this paper, we focus on both the representation of tide signals by GNSS water level height observations and suitable methods for effective filtering of GNSS heights in order to separate the tidal signature from shorter term variations (e.g. wave and dynamic draft variations and observation noise). Spectral analysis based on the Fourier transform is used to analyze the tide signature contained in both the GNSS heights and tide gauge data. Based on the determination of the main tidal harmonic constituents (M2, S2, K1, and O1) from the unfiltered and filtered time series, we assess the Savitzky-Golay and Gaussian low-pass filters for their ability to reduce short-term water level variations while retaining the underlying tide signal as much as possible.

2. GNSS DATA CAPTURE AND PROCESSING

For this study, a GNSS receiver was installed in August 2011 by Fugro Survey Pty. Ltd, Australia on a floating pontoon at Hillarys Boat Harbour located on the Western Australian coast (Figure 1). The pontoon was newly contracted and not in service at the time of observation and as such no vessel has been moored to it. As the pontoon was located in a protected harbor area (e.g. controlled environment), effects due to sea swell and vessel motion were largely reduced.

A high-performance Trimble Zephyr Geodetic antenna was connected to a Fugro Starpack GNSS receiver, which included an internal Trimble BD982 engine (Fugro, 2014). GPS and GLONASS carrier phase observations on the L1 and L2 frequencies were recorded continuously for 30 days from August 1st to August 31st, 2011 at 1 Hz sampling rate. The 1 Hz

GNSS data were processed and resampled to 1 minute to compare it with the tide gauge observations installed at the same site which was provided as 1-minute.

The International GNSS Service (IGS) station CUT0, comprising a Trimble GNSS receiver at Curtin University, located approximately ~25 km from the GNSS water level height station at Hillarys was used as a Reference Station (RS). The commercial software package Trimble Business Centre (TBC) was used to process the GNSS data in a post-processed kinematic (PPK) solution.



Figure 1. Hillarys Tide Gauge (red circle) and GNSS water level height station (yellow circle) [Fugro, 2014].

3. RELATION BETWEEN TIDE GAUGE AND GNSS HEIGHTS

For comparison with GNSS water level heights, the record of the SeaFrame tide gauge station at Hillarys Boat Harbor operated by the National Australian Tide Gauge Network was used (PCTMSL, 2007). The tide gauge was located 348 m southeast of the GNSS water level height station (see Figure 1). Originally observed at 1 Hz, the tide gauge observations are provided as 1-minute average values.

Before direct comparison, it is important to reduce GNSS water level height and tide gauge observations are reduced to a common datum at Hillarys. While GNSS water level heights are computed as ellipsoidal heights relative to the WGS84 ellipsoid, the traditional tide gauge heights are relative to chart datum. In this study, the Australian Height Datum (AHD) was used as the reference datum for both heights obtained from the GNSS and tide gauge station observations. The AHD is the vertical datum used in Australia and its zero level is based on mean sea level observed at 32 tide gauge stations located around Australia (Roelse, Granger, & Graham, 1971).

At the location of the GNSS antenna, the height difference between the ellipsoidal height and AHD height denoted as $N_{GNSS\ Tide}$, was computed using the AUSGeoid09 model, which is

accurate to ~ 0.03 m across most of Australia (Brown, 2011). This ellipsoid-geoid separation was added to all processed GNSS water level observations denoted as $h_{GNSS\ Tide}$ to convert them to AHD heights, e.g. $GNSS_{Tide\ AHD}$ (see Figure 2). In addition, the antenna offset (A_{offset}) between the GNSS antenna Phase Centre (APC) and waterline (WL) measured as 3.418 m was subtracted from all GNSS water level observations such that:

$$GNSS_{Tide\ AHD} = h_{GNSS\ Tide} - A_{offset} - N_{GNSS\ Tide} \quad (1)$$

Observations at the tide gauge stations are referred to the chart datum at Hillarys denoted here as $Tide\ Obs_{CD}$ as shown in Figure 2. The offset (CD_{offset}) between the chart datum and AHD at the Hillarys tide gauge station was -0.763 m (BOM, 2015; cf. Figure 2). This offset was added to all records to shift the tide gauge heights relative to AHD as depicted in Figure 2, where:

$$Tide\ Gauge_{AHD} = Tide\ Obs_{CD} + CD_{offset} \quad (2)$$

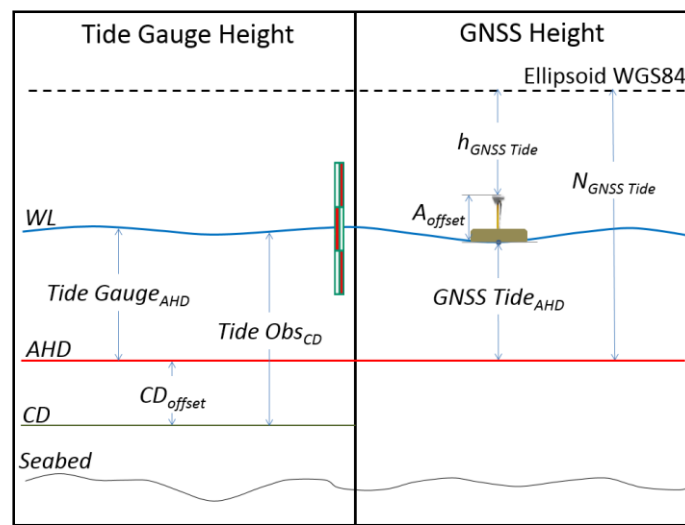


Figure 2. Datum connections between GNSS water level and tide gauge observations.

To evaluate the quality of the GNSS water level height estimates referred to AHD (cf. Equation 1), a direct comparison with tide gauge observations referred to AHD (cf. Equation 2) was performed. Overall the comparison between the GNSS water level heights and tide gauge heights showed a good agreement as illustrated in Figure 4. Furthermore, the GNSS water level height and tide gauge height time series were highly correlated as demonstrated by a correlation coefficient of 0.98. The good agreement was also verified by a root-mean-square (RMS) value of the differences of 0.0325 m. Moreover, the differences between the GNSS water level heights and tide gauge heights had a standard deviation of 0.029 m and a mean of -0.0143 m. The small mean value is within the accuracy estimate of the geoid-ellipsoid separation of 0.03 m, thus demonstrating that there is no significant bias between both time series.

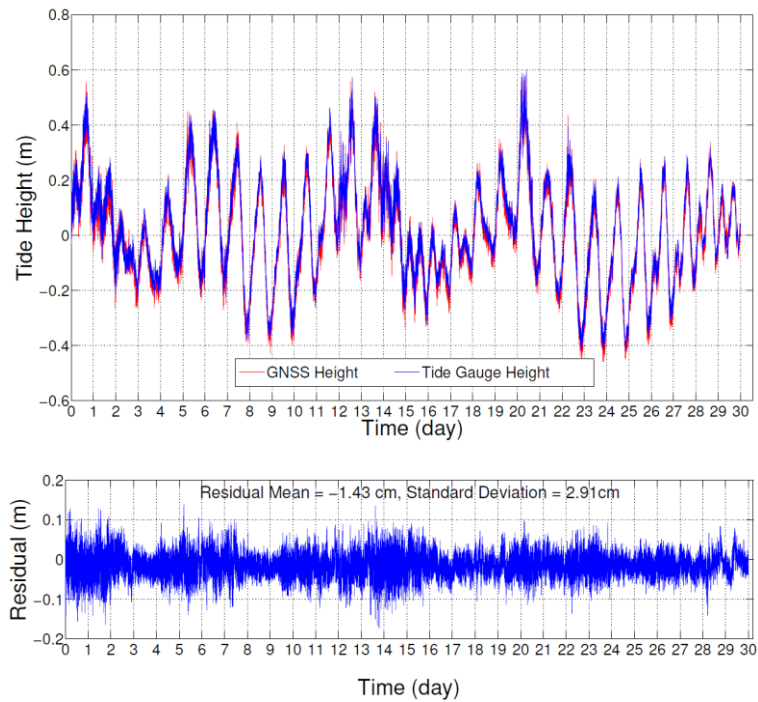


Figure 3. Top: Comparison between GNSS water level heights (red) and tide gauge heights (blue) measurements. Bottom: Difference between both heights.

4. SPECTRAL ANALYSIS

In this study, spectral analysis based on the Fourier Transform was used to calculate the amplitude (e.g. energy) of the most dominant tidal harmonic constituents (e.g. M2, S2, K1, and O1) that represent a combination of the lunar and solar tide. Each time series was transformed to its frequency spectrum using the Fast Fourier Transform (FFT) from which the tidal harmonic constituents was extracted. The respective frequency spectra illustrated in Figure 4, clearly show that both the GNSS water level and tide gauge signals were dominated by the daily (K1 and O1), and half-daily (M2 and S2) tidal harmonic constituents. Therefore, we analyse here only these harmonic components as a good representation for short-term tidal variations at the study site.

The amplitudes of the tidal harmonic constituents as extracted from the respective frequency spectra were almost identical (at the mm-level) as shown in Table 1. From Table 1, it can also be seen that the tidal signal at the test site was dominated by a diurnal variation. In addition, the agreement of the amplitudes derived from the GNSS water level and tide gauge heights was slightly better for the semi-diurnal constituents (~1 mm) than for the diurnal constituents (~2 mm).

Constituents	Period (hrs)	Amplitude (m)	
		GNSS height	TG Height
M2	12.421	0.0556	0.0563
S2	12.000	0.0538	0.0527
K1	23.934	0.1180	0.1163
O1	25.819	0.1148	0.1125

Table 1. Periods and amplitudes of the major tidal harmonic constituents extracted from the GNSS water level height and tide gauge height signals.

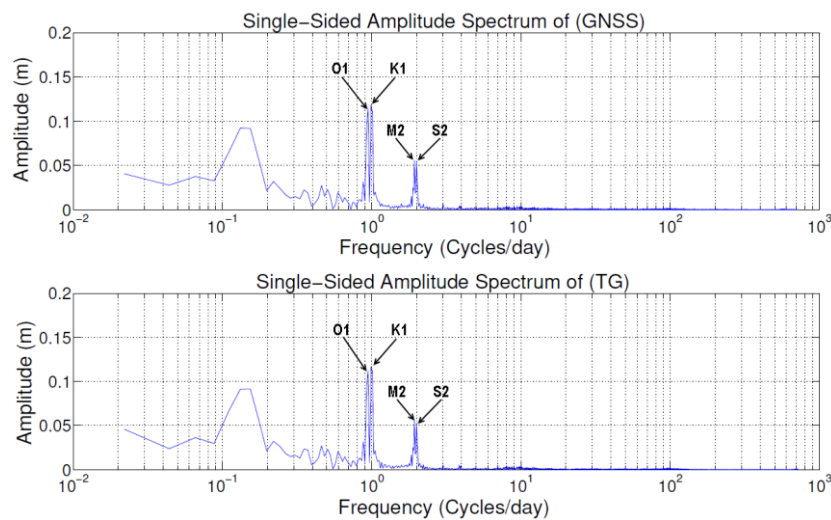


Figure 4. Single-sided frequency spectrum of GNSS water level heights (Top) and tide gauge heights (Bottom)

5. FILTERING METHODS

The tidal signals (e.g. extracted from GNSS and tide gauge heights) contain low- and high-frequency variations. The high frequency may predominantly be caused by the wave, dynamic draft variations and measurement uncertainties during the data collection. These higher frequency variations are considered here as noise when focusing on the low-frequency tidal signals with semi-diurnal and diurnal periods. To extract the low-frequency tide signal and eliminate the high-frequency noise from GNSS height solutions, low pass filters were used, which pass low-frequency and suppress high-frequency signals from the time series.

In this study, GNSS and tide gauge heights were filtered using two filters: Savitzky-Golay and Gaussian filters. The Savitzky-Golay filter is a method of data smoothing based on least-squares polynomial approximation, and the smoothed output values are less effective at reducing noise, but more effective at retaining the shape of the original signal (Schafer, 2011). Meanwhile, the Gaussian filter is convenient because the standard deviation of the appropriate Gaussian

distribution can be related directly to the 50% frequency response of the filter (Mitchell et al., 1966). The Gaussian distribution approaches very close to zero at about three standard deviations from the mean, where 99% of the distribution falls within 3 standard deviations. This mean can normally limit of data to contain only values within three standard deviations of the mean (Fisher, 1994).

The filtering techniques were used to assess their ability to eliminate high-frequency signals while maintaining the lower frequency tidal signal. The best ideal filter would be the one that optimizes the flat amplitude response and has zero phase distortion (Wert, 2004). The flat amplitude response is important so as to prohibit any contaminating effects from entering the filtered time series. Furthermore, filter performance depends on filter length as a function of the total time series length. In this study, the filter properties were assessed by their ability to correctly recover the amplitudes of the major tidal harmonic constituents (M2 S2, K1, and O1) through spectral analysis and suppressing other high-frequency signals.

In order to evaluate the performance of the selected filters in relation to the window length, we examined both the agreement between filtered tide gauge and GNSS water level time series and the dampening (e.g. signal loss) effect on the major tidal harmonic constituents. For the former, we simply filtered both the original tide gauge and GNSS water level time series (cf. Figure 3 top) and analysed the respective differences by quantifying the standard deviation (at 95% confidence) and the maximum of the differences. To quantify the dampening effect, we only analysed the GNSS water level time series (e.g. filtered vs. unfiltered) as the tide gauge time series provided very similar results. We applied the following three-step procedure:

- (i) Extract the major tidal harmonic constituents from both the unfiltered and filtered time series.
- (ii) Reconstruct the unfiltered and filtered tidal signal based on the major tidal harmonic constituents from step (i) by superposing the harmonic signals.
- (iii) Analyse the differences between the unfiltered and filtered reconstructed tidal signal from step (ii) by quantifying the standard deviation (at 95% confidence) and maximum of the differences.

Importantly, any differences between the reconstruct the unfiltered and filtered tidal signal present in step (ii) are only due to the application of the filter with the selected window length. Therefore, the difference in step (iii) can be used to assess the filters performance.

As an example, the frequency spectrum for the smoothed GNSS water level heights after applying the Savitzky-Golay and Gaussian filters with a window length of 100 minutes is shown in Figures 5 and 6, respectively. Similar to the unfiltered signal (cf. Figure 4), the frequency spectrum clearly depicts the four major tidal harmonic constituents. Both Figures 5 and 6 also include the frequency spectrum of the differences between the filtered and unfiltered tide signals, which clearly documents the low-pass filter properties by suppressing high-frequency signals and leaving low-frequency signals largely unchanged.

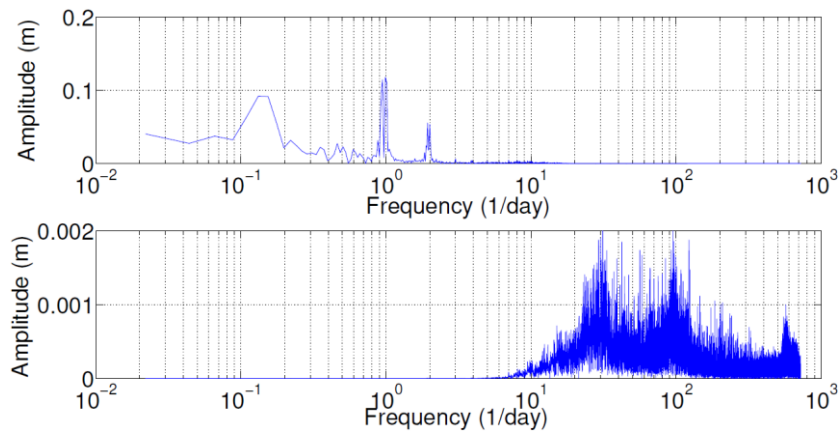


Figure 5. (Top): Single-sided frequency spectrum of the GNSS water level height signal smoothed by the Savitzky-Golay filter with a 100-minute window length. (Bottom): Single-sided amplitude spectrum of the differences between the filtered and unfiltered GNSS water level height signal.

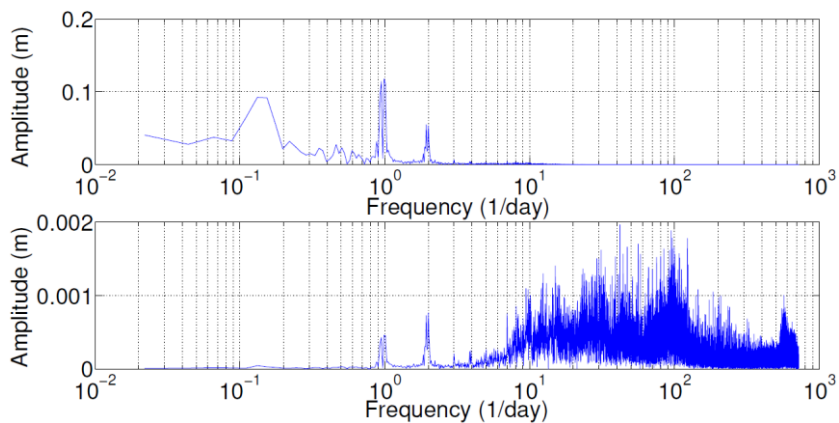


Figure 6. Top: Single-sided frequency spectrum of the GNSS water level height signal smoothed by the Gaussian filter with a 100-minute window length. Bottom: Single-sided amplitude spectrum of the differences between the filtered and unfiltered GNSS water level height signals.

While the Savitzky-Golay filter does not show any low-frequency signals in the residuals (cf. Figure 5) the Gaussian filter instead shows some residual amplitudes coinciding with the four major tidal harmonic constituents. This indicates that the corresponding amplitudes of the filtered signal were altered (damped) with respect to the unfiltered signal. This damping property was assessed in more detail by applying a series of different window lengths (10, 30, 60, 80, 100, 120, 150, 180, 220, 260, 300 and 360 minutes), all considerably shorter than the target periods (e.g. diurnal and semi-diurnal). The results for the Savitzky-Golay and Gaussian filters are shown in Figure 7.

Both filters showed a rather similar behaviour for the differences between filtered GNSS and tide gauge water level time series. Both the deviation of the differences and maximum differences decreased with increased window length, demonstrating that a large part of the differences was indeed caused by higher-frequency variations. However, analysing differences

between the filtered and unfiltered GNSS water level time series (cf. three-step procedure above) revealed some significant differences in terms of dampening the amplitudes of the four major tidal harmonic constituents. It can be clearly seen that the dampening effect was considerably smaller for the Savitzky-Golay with a standard deviation of the differences and maximum difference of only 2 mm and 2.3 mm, respectively, for the longest window length of 360 minutes considered here. For shorter window lengths, the values were at or below the mm-level, thus could be safely neglected for practical applications. In contrast, the Gaussian filter exhibited considerably larger dampening effects. The standard deviation of the differences and maximum differences were well above the mm-level even for rather short window lengths and reached maximum values of 19 mm and 25 mm, respectively, for a 360-minutes window length. Hence, especially for longer window lengths, these dampening effects cannot be neglected.

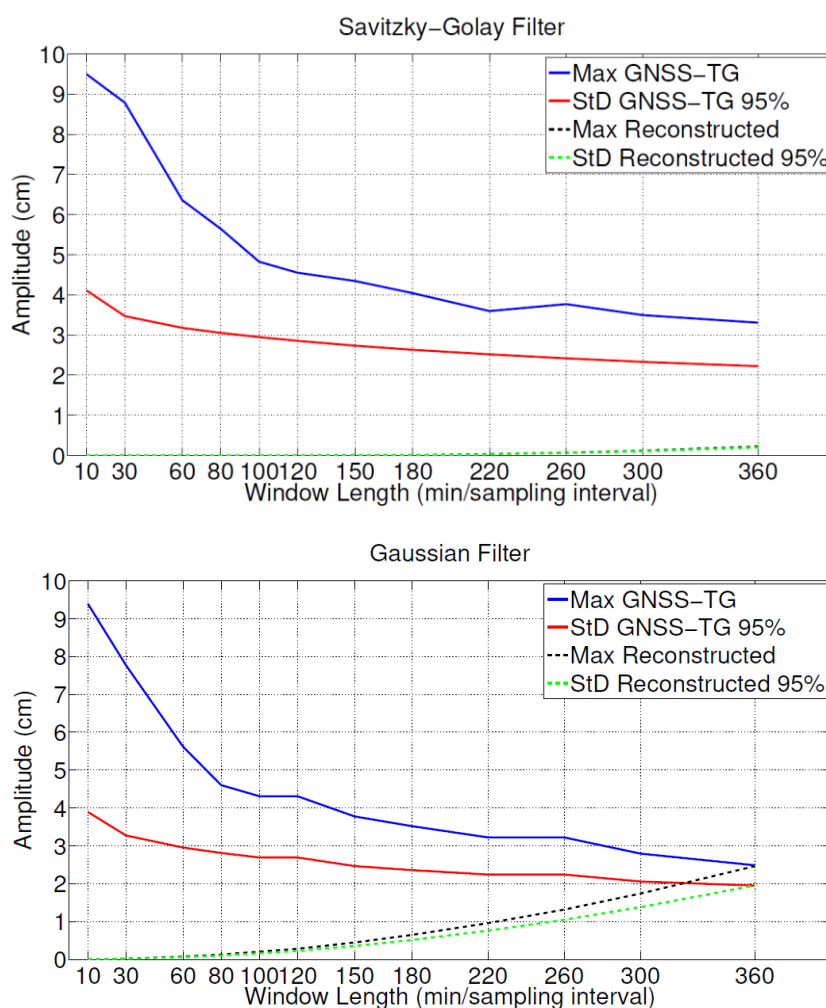


Figure 7. Performance of the Savitzky Golay filter (Top) and Gaussian filter (Bottom) in relation to various window lengths used. Differences between the filtered GNSS water level and tide Gauge time series are denoted by GNSS-TG and are shown by solid lines. Dampening effects as manifested in the reconstructed tide signals are shown by dotted lines. The standard deviations are given to a 95% confidence level.

6. CONCLUSION

This study demonstrated that there is good agreement between GNSS water level and tide gauge heights. While the GNSS water level heights were slightly noisier (with some more outliers) than the tide gauge heights, their RMS-agreement was 0.0325 m with a very high correlation coefficient of 0.98. Furthermore, we demonstrated that the tide signal at Hillarys Boat Harbour was dominated by the four major tidal harmonic constituents (M2 S2, K1, and O1) during the 30-day period considered in this study.

Both the Savitzky Golay and Gaussian filters showed their ability to extract low-frequency tide variations and suppress high-frequency signals. However, the Savitzky Golay filter was found to better preserve the low-frequency tidal harmonic constituents with dampening effects of only a few mm for a rather long window length of 360 minutes. Meanwhile, the Gaussian filter demonstrated stronger smoothing that led to increased dampening of the low frequency tidal harmonic constituents. In the extreme case of a 360-minute window length, the standard deviation of the differences and maximum differences of the reconstructed tide signals using M2 S2, K1, and O1 were 19 mm and 25 mm, respectively.

While dampening effects through the Savitzky Golay filter can safely be neglected, they should not be ignored for the Gaussian filter using longer window lengths. However, both filters maximum effects still remained below the 5 cm level (95% confidence), which would meet current IHO standards for a Special Order Survey. Nonetheless, it has to be pointed out that the studied dampening effects when filtering GNSS-derived tide heights may not be the only error source in the extracted tide signal. For example, errors in the geoid undulation value, required when the tide is expressed with respect to the chart datum, could easily be much larger, though would be at an acceptable level for the study site.

ACKNOWLEDGEMENTS. We are grateful for Fugro Survey Pty Ltd., Western Australia for providing the GNSS observation and tide gauge data used in this study. Faisal Alsaq is grateful to King Abdul-Aziz University, Saudi Arabia, for his PhD funding.

REFERENCES

- Capuano, P., De Lauro, E., De Martino, S., & Falanga, M. (2011). Water-level oscillations in the Adriatic Sea as coherent self-oscillations inferred by independent component analysis. *Progress in Oceanography*, 91(4), 447-460.
- Dodd, D., Mills, J., Battilana, D., & Gourley, M. (2010). *Hydrographic surveying using the ellipsoid as the vertical reference surface*. Paper presented at the Proceedings of the FIG Congress.
- Doodson, A. T. (1928). The analysis of tidal observations. *Philosophical Transactions of the Royal Society of London. Series A, Containing Papers of a Mathematical or Physical Character*, 227, 223-279.
- Ducarme, B., Venedikov, A., Arnosó, J., & Vieira, R. (2006). Analysis and prediction of ocean tides by the computer program VAV. *Journal of Geodynamics*, 41(1), 119-127.
- Fisher, R., Perkins, S., Walker, A., & Wolfart, E. (1994). Hypermedia image processing reference. *Department of Artificial Intelligence, University of Edinburgh*.
- Flinchem, E., & Jay, D. (2000). An introduction to wavelet transform tidal analysis methods. *Estuarine, Coastal and Shelf Science*, 51(2), 177-200.
- Fugro, (2014). Hillary's GNSS Tide Trials, Technical note V3, Fugro survey Pty. Ltd. Western Australia, 2014.
- IHO (International Hydrographic Organization) (2005) Manual on Hydrography. Publ. No. M-13. 1st edn. Monaco. <http://www.iho.shom.fr>
- Jay, D. A., & Kukulka, T. (2003). Revising the paradigm of tidal analysis—the uses of non-stationary data. *Ocean Dynamics*, 53(3), 110-125.
- Kopparapu, S., & Satish, M. (2014). Optimal Gaussian Filter for Effective Noise Filtering. *arXiv preprint arXiv:1406.3172*.
- Lam, R. K. (1974). Atoll permeability calculated from tidal diffusion. *Journal of Geophysical Research*, 79(21), 3073-3081.
- Mills, J., & Dodd, D. (2014). Ellipsoidally referenced surveys for hydrography. Publ. No 62. International Federation of Surveyors (FIG) .
- Press, W. H., & Teukolsky, S. A. (1990). Savitzky-Golay Smoothing Filters. *Computers in Physics*, 4(6), 669-672.
- Pytharouli, S., & Stiros, S. (2012). Analysis of short and discontinuous tidal data: a case study from the Aegean Sea. *Survey Review*, 44(326), 239-246.
- Roelse, A., Granger, H., & Graham, J. (1971). The adjustment of the Australian levelling survey—1970–71: Report 12. *National Mapping Council*.

- Sakamoto, Y., Ishiguro, M., & Kitagawa, G. (1986). Akaike information criterion statistics. Dordrecht, The Netherlands: D. Reidel.
- Schafer, R. W. (2011). What is a Savitzky-Golay filter?[lecture notes]. *IEEE Signal Processing Magazine*, 28(4), 111-117.
- Tay, S., Coatanhay, A., Maussang, F., & Garello, R. (2010). *A tracking algorithm for GNSS reflected signals on sea surface*. Paper presented at the Geoscience and Remote Sensing Symposium (IGARSS), 2010 IEEE International.
- Thompson, R. O. (1983). Low-pass filters to suppress inertial and tidal frequencies. *Journal of Physical Oceanography*, 13(6), 1077-1083.
- Venedikov, A. P., Arnosó, J., & Vieira, R. (2005). New version of program VAV for tidal data processing. *Computers & geosciences*, 31(5), 667-669.
- Wert, T. D., Dare, P., & Clarke, J. H. (2004). *Tidal height retrieval using globally corrected GPS in the Amundsen Gulf region of the Canadian Arctic*. University of New Brunswick, Department of Geodesy and Geomatics Engineering.

CONTACT

Faisal Alsaq
 Ph.D. candidate
 Department of Spatial Sciences
 Curtin University
 GPO Box U 1987, Perth WA 6845,
 Australia
 Tel: +966502027711
 Email:
faisal.alsaq@postgrad.curtin.edu.au

Michael Kuhn
 Associate Professor, MSc (Geospatial
 Science) Coordinator
 Department of Spatial Sciences
 Curtin University
 GPO Box U 1987, Perth WA 6845,
 Australia
 Tel: +618 9266 7603
 Email: m.kuhn@curtin.edu.au

Ahmed El-Mowafy
 Associate Professor, GNSS Positioning
 and Navigation
 Coordinator of Graduate Studies
 (Research)
 Department of Spatial Sciences
 Curtin University
 GPO Box U 1987, Perth WA 6845,
 Australia
 Tel: +61 8 9266 3403
 Email: a.el-mowafy@curtin.edu.au

Paul Kennedy
 Deputy Managing Director, Fugro Survey
 Pty Ltd
 24 Geddes St, Balcatta
 Western Australia 6021
 Tel: +61 8 6477 4400
 Email: p.kennedy@fugro.com